

## INTEGRATED OPTIC DISTRIBUTED BRAGG REFLECTOR FABRY-PEROT MODULATOR FOR MICROWAVE APPLICATIONS\*

W. J. Zubrzycki<sup>†</sup>, B. V. Borges<sup>†</sup>, P. R. Herczfeld<sup>†</sup>,  
 S. H. Kravitz<sup>\*</sup>, G. R. Hadley<sup>\*</sup>, G. A. Vawter<sup>\*</sup>, R. F. Corless<sup>\*</sup>, R. E. Smith<sup>\*</sup>, J. R. Wendt<sup>\*</sup>, J. C. Word<sup>\*</sup>, and  
 T. M. Bauer<sup>\*</sup>

<sup>†</sup>Center for Microwave-Lightwave Engineering, Drexel University, Philadelphia, PA 19104

and

<sup>\*</sup>Sandia National Laboratories, Albuquerque, NM 87185-0603

### ABSTRACT

An integrated optic Fabry-Perot modulator is considered. The device, fabricated on III-V materials, uses distributed Bragg reflectors as mirrors. The greatest technical challenge in the realization of this device was the fabrication of the gratings with nanometer feature sizes. First order gratings 0.09  $\mu\text{m}$  in width and of 0.8  $\mu\text{m}$  in depth were written on a 2  $\mu\text{m}$  wide rib waveguide and successfully etched. The design, fabrication, and performance of the device is discussed.

### INTRODUCTION

External modulators are gaining popularity in high speed fiber optic links. At first, most modulators were fabricated on LiNO<sub>3</sub> substrates utilizing a Mach-Zehnder interferometer (MZI) layout. Increasingly the choice of materials are III-V compounds (GaAs, InP) raising the prospect of chip level integration of integrated optics circuitry (modulator) and the high speed monolithic microwave integrated circuits (MMIC), thus improving performance while reducing cost.

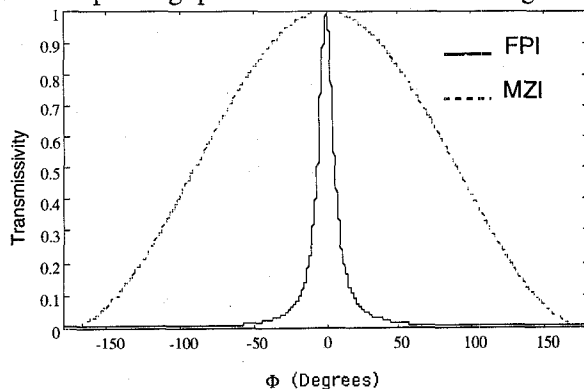


Figure 1. Transmissivity v.s. phase angle of ideal Fabry-Perot and Mach-Zehnder interferometers.

Problems with the Mach-Zehnder type modulators include high driving voltages, large size, and complex electrode structure to compensate for the velocity mismatch of the light and microwaves. One alternate approach, explored in this paper, is the use a Fabry-Perot interferometer (FPI) with internal distributed

mirrors (gratings). The transfer function of an ideal (lossless) MZI and a FPI with 90 percent reflective mirrors is shown in Fig. 1, illustrating that the FPI requires far less phase change than the MZI, resulting in a smaller device and/or lower driving voltage.

A high performance FPI presents the following requirements: high mirror reflectivity and low losses in the cavity (i.e. high finesse), short cavity and grating length (high speed), and high figure of merit (low driving voltage). In this paper we describe the design, fabrication and preliminary results of an FPI modulator. Problems with the initial design and the subsequent redesign of the device will be discussed.

### DESIGN OF THE FABRY-PEROT MODULATOR

The semiconductor epitaxial structure, with a rib optical guide etched into the p cladding as shown in Fig. 2, served as the basis for the design. This particular structure was adopted because it has been successfully used in conjunction with related projects at Sandia and was readily available [1, 2]. It has a GaAs p-n junction in the guiding layer which exploits the linear and quadratic electro-optic effects, as well as the plasma, band filling, and band shrinkage effects to yield a high figure of merit (FOM) of 60°/V·mm. To obtain highly reflective mirrors (80%), first order gratings with a pitch of 0.18  $\mu\text{m}$  were required for a free space wavelength of 1.3  $\mu\text{m}$ . Considering a fifty-percent duty cycle, the desired etch width is 0.09  $\mu\text{m}$ . To attain a large coupling coefficient, a grating etch depth of 0.8  $\mu\text{m}$  and a grating length of 65  $\mu\text{m}$  was required. The design called for a cavity length of 200  $\mu\text{m}$  and a driving voltage below 5 volts. In this particular structure the upper and lower clads are comprised of GaAlAs with a 40 percent Al concentration, but the upper clad is p-type and the lower one is n-type which is necessary to produce the required electric field pattern. This arrangement provides for optically symmetric, but electrically asymmetric cladding layers.

Fig. 2a shows the crosssection (right half) normal to the direction of the beam propagation depicting the rib guide etched into the upper cladding. The crosssection in the direction of the propagation, including the Fabry-Perot cavity formed by the grating reflectors, is shown in Fig. 2c. All the pertinent material and geometric information for this III-V epitaxial structure is summarized in Fig. 2b.

TU  
4C

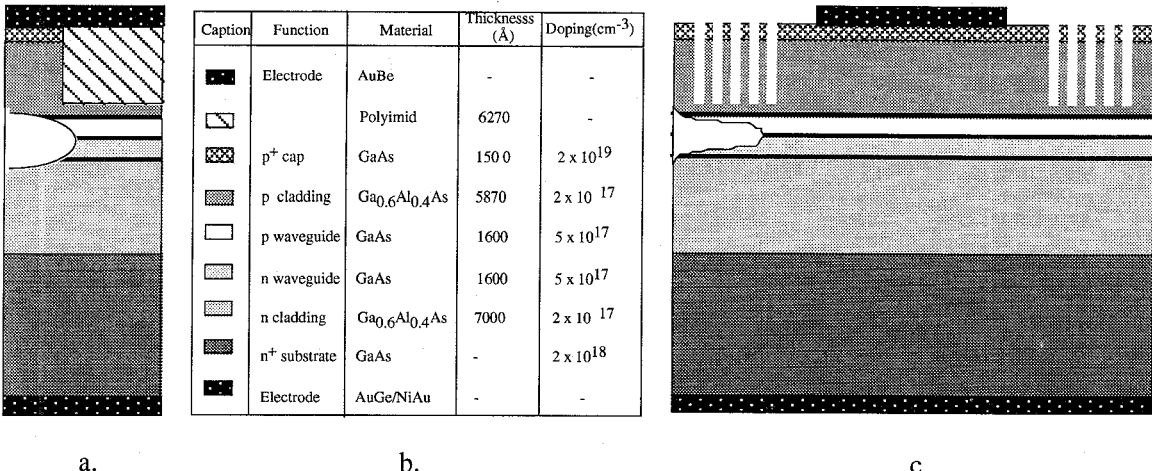


Figure 2. Epitaxial structure of Fabry-Perot modulator, with a.) transversal, c.) longitudinal crossections and b.) identification of thicknesses and material characteristics of the layers.

### INITIAL DEVICE FABRICATION PROCESS

The greatest technical challenge in the realization of this device was the fabrication of the gratings with nanometer feature sizes. State-of-the-art fabrication processes began with the rib waveguide etch. Rib waveguides were patterned on the semiconductor wafer using standard optical lithography techniques then etched in a reactive ion beam etching system (RIBE). Following the rib waveguide etch, a tri-level mask was deposited on the wafer and gratings were directly written on the waveguides using a JEOL JBX-5FE Electron Beam Lithography System. The tri-level mask consisted of 3500Å of photoresist, followed by 250Å of titanium, and 1700Å of polymethylmethacrylate (PMMA) electron beam photoresist. The gratings were then etched in the RIBE and inspected in an electron microscope. Fig. 3 shows a cross section of deep gratings showing the anisotropic sidewalls etched in the RIBE attesting that the first order gratings were successfully constructed with the stringent feature sizes described above. Following the grating etch, polyimide was spun and cured on the top surface to provide a level vehicle for the p-type AuBe top contact. The sample was then lapped to a total thickness of 150µm to facilitate cleaving and a Au/Ge/Ni/Au contact was deposited on the bottom. Fabrication was completed with the annealing of the contacts.

### INITIAL RESULTS

The optical waveguides without gratings displayed well confined light at the output. Devices with gratings, however, indicated a total loss of confinement. A two-dimensional finite difference solution to the eigenmode equation was used to investigate the mode shape under the gratings. Simulations revealed that the symmetric cladding arrangement provides for good confinement of the optical beam under the rib guide (Fig.4). However, the deep gratings etched into the rib significantly reduce its index as seen by the



Figure 3. Cross section of anisotropically etched deep first order gratings at 1.3µm. Grating depth is 800nm and grating etch width is 90nm.

propagating mode. As a result, the optical field redistributes to the lower cladding and spreads into slab modes, with an effective loss of confinement.

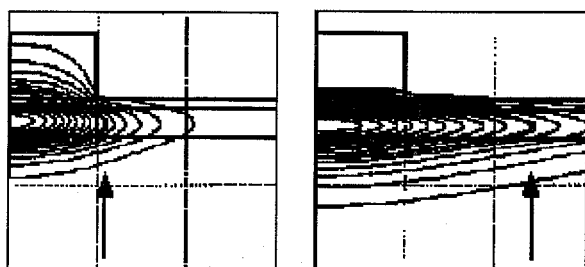


Figure 4. Well confined mode shape under the unperturbed rib waveguide (left) and the unconfined mode under the rib with the grating perturbation (right). Arrow indicates lateral extreme of the 1/e spot size.

## REDESIGN OF THE FABRY-PEROT MODULATOR

The redesign focused on optimizing the confinement and coupling coefficient by varying the grating depth and the refractive indices of the upper and lower clads. The refractive indices of the claddings were controlled by adjusting the aluminum concentration of the GaAlAs material and were calculated based on the Aframovitz method [3]. The notion is that shallower gratings and a smaller index of the lower cladding will eliminate the redistribution of the field into slab modes, and thus preserve confinement.

Numerical simulations were used to study the mode shape and light intensity distribution for different grating depths and varying aluminum concentrations in the cladding layers.

The overlap integral [4] of the unperturbed mode (no grating) and the perturbed (grating) mode, a measure of the light coupled between these modes caused by the discontinuity of the grating region, was used to quantify confinement. An overlap of 1.0 infers unperturbed transmission, while values less than one imply scattering and some loss of confinement. For example, the earlier design discussed above had an overlap of 0.8, which is clearly insufficient as it did not provide confinement. An overlap of 0.95 or higher is desirable.

The coupling coefficient was calculated according to Agrawal [5] and is plotted together with the overlap integral in Fig. 5 as a function of the grating depth. Coupling coefficients determined analytically were in agreement with those calculated numerically using a three dimensional Alternate Direction Implicit (ADI) solution to the scalar wave equation [6]. Simulations showed that an asymmetric aluminum concentration of 40% in the upper cladding and 60% in the lower cladding concentrated the mode in the waveguide layer and at the bottom of the gratings. The optimum grating depth was found to be  $0.677\mu\text{m}$  with a rib height of  $0.777\mu\text{m}$ . The  $0.1\mu\text{m}$  of unetched rib under the gratings greatly increases the confinement of the light as compared to the deep gratings etched completely through the rib in the first design, Fig. 6. Therefore, the overlap was improved from 0.80, which was obtained in the initial design, to 0.95 for the current configuration. The coupling coefficient for this optimized condition was calculated to be  $100\text{ cm}^{-1}$  requiring a grating length of  $150\mu\text{m}$  for 80% reflective mirrors. The required grating pitch was found to be  $0.2011\mu\text{m}$ .

### MODIFIED FABRICATION TECHNIQUE.

The initial grating processing proved successful, but, the use of a tri-level mask did not provide a planar surface for the PMMA and the thin mask layers often resulted in rounded rib profiles. The present process involves spinning on  $10000\text{\AA}$  Polymethylglutarimide (PMGI) followed by an oven bake at  $270^\circ\text{C}$  which planarizes and hardens that material. Next,  $1800\text{\AA}$  of plasma enhanced chemical vapor deposition (PECVD)  $\text{SiO}_2$  is deposited, followed by a final layer of PMMA  $1700\text{\AA}$  thick. PMMA is then patterned with the gratings and used to etch the  $\text{SiO}_2$ . The  $\text{SiO}_2$  layer is used to

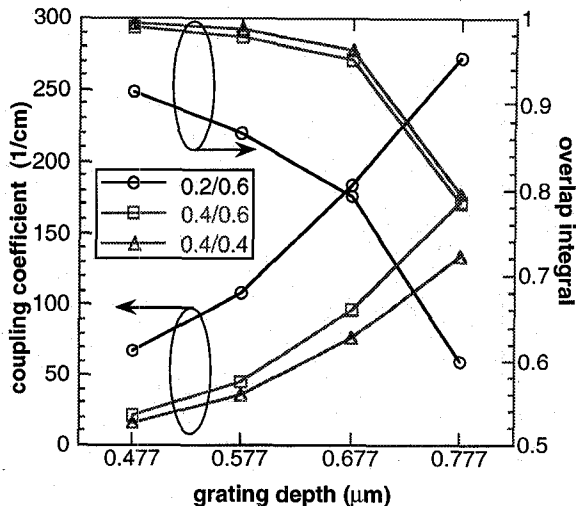


Figure 5. Coupling coefficient and overlap integral as a function of grating depth. Legend is in the form upper/lower clad Al concentration (e.g. 0.2/0.6 represents 20% Al in upper clad and 60% in lower clad). The rib height is  $0.777\mu\text{m}$ .

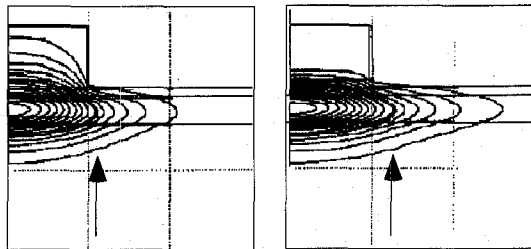


Figure 6. Mode shapes of redesigned device. Well confined mode under rib on left, as well as under gratings, on right.

define the PMGI in an oxygen RIBE etch. The remaining thick mask of  $\text{SiO}_2$  and PMGI is used to etch the gratings in the RIBE. Upon completion of the grating etch, the PMGI is stripped in *n*-methylpyrrolidone (NMP). This is an advantage over the initial design. The hardened photoresist of the initial processing method could not be stripped in any organic solvent, it had to be etched away in an oxygen RIE. Fig. 7 shows the gratings on a test wafer after the PMGI has been stripped. The thick planar layer of PMGI allows deep grating etches without eroding the corners of the rib, thus resulting in a squared post-grating etched rib. The rib waveguide and remaining device processing remains the same.

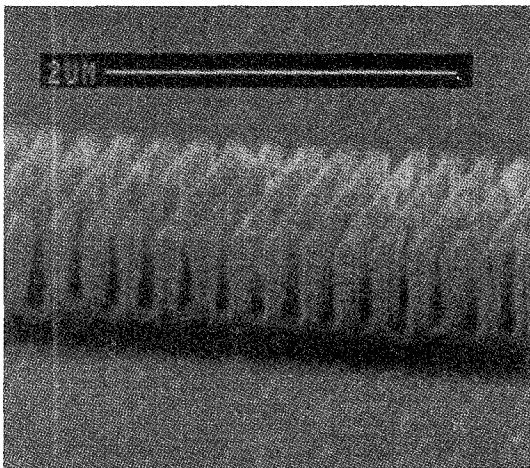


Figure 7. Electron micrograph of grating etched across 2.0 $\mu$ m rib waveguide.

### CONCLUSION

This paper is concerned with the development of a novel modulator in GaAs that utilizes a Fabry-Perot resonant cavity. Highly reflective distributed Bragg reflectors served as mirrors for this device. Our first design and fabrication utilized available technology and materials. We successfully fabricated state-of-the-art first order gratings with a pitch of 0.18 $\mu$ m and depth of 0.8 $\mu$ m. However, we found the deep gratings destroyed lateral confinement which led to a redesign of the structure. The redesign focused on optimizing the confinement and coupling coefficient by varying the grating depth and the refractive indices of the upper and lower clads. Numerical simulations were used to study the mode shape and light intensity distribution for different grating depths and aluminum concentrations in the cladding layers. A slightly shallower grating depth and asymmetric Al concentration greatly increases confinement while maintaining a large coupling coefficient. New mask configurations were developed to etch the gratings.

### ACKNOWLEDGMENT

This work was supported in parts by the US Army under contracts DAAL-01-92-K-0230, DAAL-03-92-G-0066, by NSF grant INT-900-22-89 and the Brazilian Research Council (RHAE/CNPq).

\*This work was supported by the United States Department of Energy under Contract DE-AC04-94AL85000

### REFERENCES

- [1] Vawter, Klem, Hadley, and Kravitz, "Highly accurate etching of ridge waveguide directional couplers using in situ reflectance monitoring and periodic multilayers", *Appl. Phys. Lett.* 62 (1), 4 January 1993.
- [2] Kravitz, Hadley, Warren, Wendt, Word,

Corless, Carson, Armendariz, and Hammons, "Waveguide-to-fiber coupling using a second-order grating and an anamorphic binary optic", *Proceeding LEOS 6th Annual Meeting*, p. 472, San Jose, CA., Nov.15-18, 1993.

- [3] Afromowitz, "Refractive index of Ga<sub>1-x</sub>Al<sub>x</sub>As", *Solid State Commun.* 15 (1) 1974
- [4] Hunsperger. *Integrated Optics: Theory and Technology*, Springer Series in Optical Sciences, Vol. 33, 1982
- [5] Agrawal and Dutta. *Long-Wavelength Semiconductor Lasers*, New York: Van Nostrand Reinhold Co., 1986
- [6] Hadley, To be published